

Geometry and unoccupied electronic states of Ba and BaO on W(001)

A. Lamouri

NASA Lewis Research Center, 21000 Brookpark Road, Cleveland, Ohio 44135

W. Müller

Anatom Inc., 29904 Sycamore Oval, Westlake, Ohio 44145

I. L. Krainsky

NASA Lewis Research Center, 21000 Brookpark Road, Cleveland, Ohio 44135

(Received 19 October 1993; revised manuscript received 23 March 1994)

A study aimed at understanding the geometrical and electronic properties of barium and oxygen coadsorbed on the tungsten (001) surface has been carried out by means of work-function measurements ($\Delta\phi$), Auger-electron spectroscopy, low-energy electron diffraction, inverse photoelectron spectroscopy, and relativistic-electronic-structure calculations. A report of the experimental measurements and a comparison with theoretical results from embedded-cluster-model calculations are presented. Our experimental studies show that the work function of the W(001) surface ($\phi=4.63$ eV) is lowered to approximately 2.3–2.4 eV by coadsorption of 1 ML of Ba and O regardless of the order of deposition of these two species. The technique of IPS in the isochromat mode was used to determine the unoccupied electronic-energy band structure for ordered $c(2\times 2)$ Ba and O layers on W(001). Several spectral features are observed above the Fermi level (E_F), which we assign to transitions into Ba and W d states. The measured two-dimensional electronic band structure is independent of the order of Ba and O deposition. Using embedded-cluster-model calculations, we investigated two possible adsorption configurations of an ordered $c(2\times 2)$ adlayer of Ba and O on W(001): “tilted,” where Ba and O are placed on alternate fourfold-hollow sites, and “upright,” where the adsorbed atoms lay above the same site with Ba outermost. The calculated densities of states for the tilted geometry show distinct peaks above E_F originating from Ba and W d orbitals and are in good agreement with the experimental results.

I. INTRODUCTION

Barium dispenser cathodes are widely used in microwave power devices because of their reliability, long life, and high current densities. At operating temperatures of approximately 1300 K, these cathodes achieve current densities of up to 100 A/cm² by maintaining a low work-function surface composed of Ba and O on a W matrix.^{1,2} It is also widely accepted that the active layer of these cathodes is composed of Ba and O that is stoichiometrically very close to BaO (Ref. 3) with a coverage for the Ba and O layers believed to be between .5 ML and 1 ML.^{4,5} However, it is not clear whether Ba and O are adsorbed as a BaO molecule or if BaO dissociates completely on the surface.^{6,7}

The lowering of the work function of transition metals by adsorption of alkaline-earth metals can be attributed to the formation of a surface-dipole layer resulting from charge transfer from the adsorbate to the substrate. Recent full-potential linearized augmented-plane-wave (FLAPW) calculations for $c(2\times 2)$ Ba overlayers on W(001),⁸ however, lead to the conclusion that, for ML coverages, the bonding is not ionic but rather metallic covalent, with the dipole layer residing in the polarized Ba valence electrons, much like for the adsorption of alkali metals on transition metals.^{9,10}

In order to understand the adsorbate-substrate interac-

tion, a thorough knowledge of the arrangement of the Ba and O adatoms on the surface is necessary. Several papers with conflicting results have been published on this subject. While some groups propose a model with a standing-up adsorption layer in which Ba is outermost,^{11,12} others produce experimental and theoretical data consistent with a more coplanar adsorption geometry where Ba and O occupy alternate fourfold-hollow sites.^{13,14} These conflicting results and the interest in understanding the mechanism of operation of thermionic dispenser cathodes have generated several research programs in the last few decades. New and improved cathodes rely heavily on these studies and on a thorough understanding of not only the geometrical but also the electronic structure of alkaline-earth oxides adsorbed on transition metals.

To date, most of the studies of the adsorption of BaO on W(001) were aimed at understanding the geometrical structure of the adsorbate. Although some of these studies dealt with the electronic structure of the BaO/W system, none have been devoted to its unoccupied electronic band structure. Only two theoretical studies of this system, the FLAPW (Ref. 13) and the cluster-model¹⁵ calculations, have been reported to date, both of which lack a thorough investigation of the unoccupied densities of states (DOS).

To carry out the research, a model surface is necessary

since actual dispenser cathode surfaces are polycrystalline and porous. In addition, their mechanism of activation and operation is complex, involving diffusion of Ba and O from the impregnant and desorption of the adsorbates from the surface. Experimental measurements by Haas, Shih, and Marrian³ have shown that a reasonable model consists of 1 ML of Ba and O on the W(001) surface. Using low-energy electron-diffraction (LEED) and work-function measurements, they established that a $c(2 \times 2)$ structure and a minimum work-function value are achieved at this coverage.

In the present work, the experimental two-dimensional band structure of the unoccupied electronic levels for 1 ML of Ba and O on W(001) is presented. The measurements are compared with embedded-cluster-model calculations.

This paper is organized as follows: First, the experimental techniques and the computational details of the fully relativistic embedded-cluster-model approach are briefly described. The experimental results are then compared with the calculated DOS. Finally, the conclusions from the present study are summarized.

II. EXPERIMENTAL TECHNIQUES

The experimental work was carried out in an all stainless-steel ultrahigh-vacuum chamber operated in the low 10^{-11} -Torr range. This system is equipped with a double-pass cylindrical mirror analyzer for Auger monitoring of the surface composition and with LEED optics for monitoring the surface structure and orientation. A detailed description of the experimental setup can be found elsewhere^{16,17} and only its most important features are described here.

Inverse photoelectron spectroscopy (IPS) measurements were performed in the isochromat mode at a photon energy of 9.8 eV by means of a photon detector designed after that of Babbe *et al.*¹⁸ and a low-energy electron gun, which was built for this experiment.¹⁹ The electron gun used a BaO cathode and was mounted at 40° relative to the detector. The angle of electron incidence was varied by rotating the sample. Count rates of several hundred counts per second were achieved with an electron-beam current of $5 \mu\text{A}$. The electron-beam angular divergence was estimated at better than 3° , giving a momentum resolution of approximately 0.1 \AA^{-1} . The overall energy resolution of the spectrometer was approximately 0.6 eV.

The W(001) crystal was cleaned in vacuum by repeated heating at 1700 K in an oxygen atmosphere of 6.0×10^{-8} Torr followed by occasional flashing at 2500 K until cleanliness was confirmed by Auger-electron spectroscopy (AES), LEED, and IPS. The target was also flashed before each deposition. Ba was deposited onto the W(001) surface from a well-outgassed Ba source provided by the Philips Company. Coverages were determined by a combination of $\Delta\phi$, LEED, and AES measurements. Accurate measurements of the work-function change were performed using the retarding field method as described in Ref. 17.

Three methods were used to prepare 1 ML of BaO on

W(001). These methods have been described in detail elsewhere.²⁰

In the first method, 1 ML of barium was adsorbed on the W(001) surface followed by exposure to 0.5 L (1 L = 1 Langmuir = 10^{-6} Torr sec) of oxygen at room temperature. The work function of W(001) ($\phi = 4.63$ eV) (Ref. 21) decreased to a minimum value of 2.29 eV at this coverage. In addition, a $c(2 \times 2)$ LEED pattern and an O to Ba Auger-line intensity ratio of 2:1 were obtained.³

In the second method, the target was exposed to 0.5 L of oxygen at room temperature before the barium deposition was performed. A work-function minimum value of 2.44 eV was obtained in this case. The room-temperature $p(4 \times 1)$ O/W(001) LEED structure was replaced by a $c(2 \times 2)$ structure at a Ba coverage corresponding to the minimum work function. The O to Ba Auger ratio was similar to the one obtained in the first method. In fact, we obtained a similar LEED structure and AES intensity ratio from BaO films on W(001), which were obtained by completely oxidizing a thick barium film and then annealing it at 1100 K for approximately 3 min, as described by Mueller *et al.*²²

In the third method, we exposed the W(001) surface to 0.5 L of oxygen at approximately 1100 K before performing the barium deposition. We obtained a work-function minimum value of 2.38 eV, in the same range as for the previous methods. In contrast to the first and second methods where a ML of Ba and O on the W(001) surface created a $c(2 \times 2)$ structure, the ML here retained the $p(2 \times 1)$ LEED structure of the first adsorbed annealed oxygen layer.

To summarize, adsorption of 1 ML of BaO reduced the work function of the W(001) surface by approximately the same amount, regardless of the Ba and O deposition order and temperature treatment. However, films obtained by annealing the O layer produced a completely different LEED pattern from those of the unannealed samples. Therefore, the relationship between the geometrical structure and the work function is not unique in this case.

In real space two adsorption geometries, tilted and upright, corresponding to the $c(2 \times 2)$ LEED pattern have been considered for the unannealed surface. By comparing our experimental measurements with the results of embedded-cluster-model calculations, the structure of Ba and O adsorbed on W(001) can be determined.

III. THEORETICAL APPROACH

We used fully relativistic embedded-cluster calculations to investigate the surface electronic structure of $c(2 \times 2)$ Ba and BaO on W(001). The computational approach employed was the Dirac-Slater scattered-wave method, which was originally developed by Yang, Rabii, and Case.²³⁻²⁵

In the fully relativistic scattered-wave method, the Dirac wave equation is solved for muffin-tin potentials. All electrons are treated self-consistently in a fully relativistic fashion. The formalism includes the mass-velocity and Darwin corrections to the energy, as well as spin-orbit interaction through the use of spin-angular,

four-component wave functions in the framework of double-group theory. Quasirelativistic calculations (without spin-orbit interaction) were carried out for comparison. Slater's statistical $X\alpha$ local-density functional²⁶ was used for the treatment of exchange and correlation effects.

The W(001) substrate was modeled with an atomic cluster consisting of 25 W atoms in two layers: a 4×4 array was used for the surface layer and a 3×3 array for the subsurface layer. A ML of Ba on W(001) was modeled by positioning the Ba atoms in the fourfold-hollow sites of the surface layer in a $c(2 \times 2)$ arrangement, resulting in a $\text{Ba}_5/\text{W}_{16}\text{W}_9$ cluster. Three different heights for the Ba atom above the W(001) surface were investigated: $z_{\text{Ba}} = 4.31a_0$, $4.50a_0$, and $4.69a_0$ corresponding to 2.28, 2.38, and 2.48 Å, respectively ($a_0 = 0.5292$ Å). For Ba and O on W(001), two different adsorption sites were considered for oxygen. In the first case, O was adsorbed in the vacant fourfold-hollow sites of the Ba/W(001) surface with $z_{\text{O}} = 2.88a_0$ and $z_{\text{Ba}} = 4.63a_0$, leading to a $\text{Ba}_5\text{O}_4/\text{W}_{16}\text{W}_9$ cluster. In the second case, O was assumed to be adsorbed directly below Ba with $z_{\text{O}} = 0.89a_0$ and $z_{\text{Ba}} = 5.38a_0$, leading to a $\text{Ba}_5\text{O}_5/\text{W}_{16}\text{W}_9$ cluster. These clusters are illustrated in Figs. 1(a) and 1(b). The Ba and O heights were those optimized by Hemstreet, Chubb, and Pickett¹³ using thin-film FLAPW calculations.

The radii of the atomic spheres for the central atoms in each layer were chosen as 88% of the sphere radii, as determined in the standard fashion from the superposition of nonrelativistic atomic charge densities.²⁷ The sphere radii of the surrounding atoms were set equal to those of the central atoms to simulate the equivalences of an extended surface. The numerical potentials of the inner atoms were converged in an environment of identical potentials for the surrounding atoms. This was accomplished by transferring the potentials from the inner to the outer atoms of the cluster at each iteration. By using this approach, the inner atoms of the cluster were em-

bedded in an additional shell of atoms that enforced a proper local environment representative of an extended surface.

Projected local densities of states were generated for the inner atoms by convoluting the calculated energies of the individual states with Gaussian functions with full widths at half maxima of 0.2 eV. The DOS shown below for Ba and BaO and W include the contributions from one central Ba, O (for BaO/W), and W atom of the top layer of the cluster. Although the unit cell for $c(2 \times 2)$ coverages contains one adatom per two tungsten atoms, the one-to-one ratio was chosen because the contributions from the atomic layers to the experimentally observed spectra are expected to decay rapidly below the uppermost adsorbed layer.

IV. RESULTS

In this section, we present the results of our experimental measurements and theoretical calculations for the adsorption of 1 ML of Ba and O on W. The IPS spectra were taken at different angles of electron incidence along the $\bar{\Gamma} \bar{\Delta} \bar{X}$ and $\bar{\Gamma} \bar{\Sigma} \bar{M}$ symmetry lines of the surface Brillouin zone (SBZ) of the clean unreconstructed W(001) surface, corresponding to the $\bar{\Gamma}' \bar{\Sigma}' \bar{M}'$ and $\bar{\Gamma}' \bar{\Delta}' \bar{X}'$ directions of the SBZ of the $c(2 \times 2)$ structure, respectively [cf. Fig. 1(c)]. The spectra along the $\bar{\Gamma} \bar{\Delta} \bar{X}$ line were taken in the (001) mirror plane and those along $\bar{\Gamma} \bar{\Sigma} \bar{M}$ were taken in the (011) mirror plane of the W(001) $p(1 \times 1)$ structure. The Fermi edge was determined from the onset of photon emission.

To derive the experimental two-dimensional band structures, the component of the wave vector of the incoming electron parallel to the surface (k_{\parallel}) was determined using the equation

$$\hbar k_{\parallel} = [2m(E_i - \phi)]^{1/2} \sin \alpha,$$

where α is the angle of electron incidence measured from the surface normal, E_i is the initial energy of the electron measured from E_F , and ϕ is the work function of the surface being studied. A value of $\phi = 2.63$ eV was used for 1 ML of Ba on W(001) and $\phi = 2.37$ eV for 1 ML of Ba and O on W(001).

A. Ba on W(001)

IPS spectra for 1 ML of Ba on W(001) along the $\bar{\Gamma} \bar{\Delta} \bar{X}$ and $\bar{\Gamma} \bar{\Sigma} \bar{M}$ directions are shown in Figs. 2(a) and 2(b), respectively. Upon adsorption of Ba, all the W(001) surface states^{16,28} seem to have been completely quenched and new features appear above E_F .

Along the $\bar{\Gamma} \bar{\Delta} \bar{X}$ symmetry line these features include two well-defined peaks located at 0.6 and 3.4 eV and two shoulders located at 2.3 and 2.7 eV above E_F . A full description of these features can be found elsewhere.¹⁷

Along the $\bar{\Gamma} \bar{\Sigma} \bar{M}$ symmetry line only two features are observed above E_F , one well-defined peak located at 0.6 eV and a broad peak near 3.4 eV. Both of these features appear only between $\alpha = 0^\circ$ and 28.5° . The peak located immediately above E_F shows a slight upward dispersion, while the one above the vacuum level (E_V) disperses

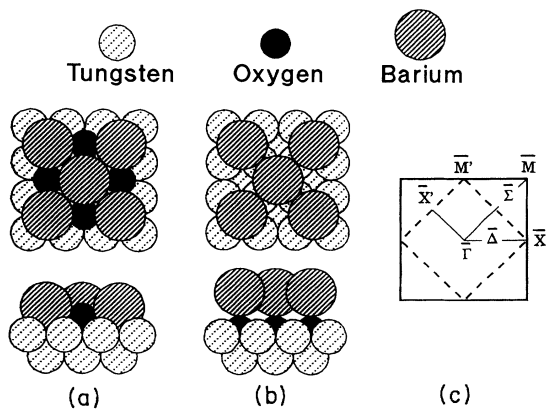


FIG. 1. Top and side views of cluster models for a $c(2 \times 2)$ ML of Ba and O on W(001) in the (a) tilted and (b) upright configurations. (c) illustrates the SBZ of the clean W(001) surface (solid square) and that of the $c(2 \times 2)$ BaO/W(001) system (dashed square).

slightly downward in this symmetry direction.

Calculated DOS for Ba heights of 2.28, 2.38, and 2.48 Å above the W substrate are shown in Fig. 3. With the exception of differences associated with states possessing energies greater than 2 eV above E_F , it is found that the DOS is changed insignificantly as the Ba height is varied. Although technically the only meaningful states associated with the calculations have energies less than the experimental vacuum level (2.7 eV), it is useful to monitor the behavior of states that have energies greater than the experimental vacuum level but smaller than the cluster vac-

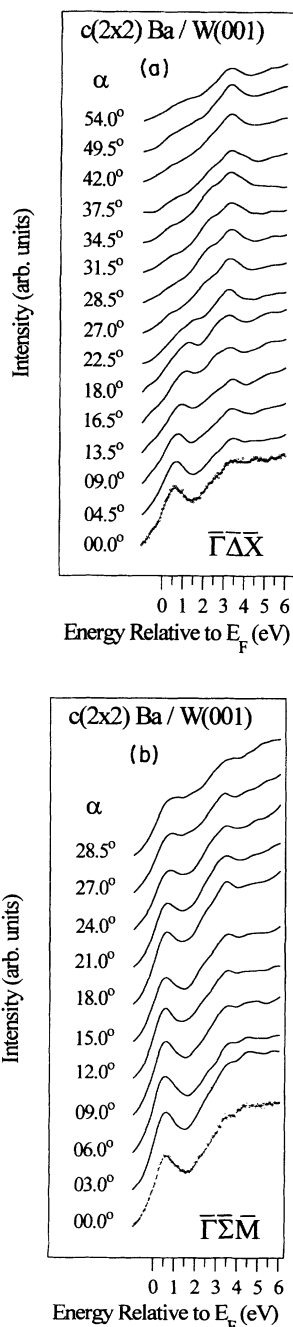


FIG. 2. IPS spectra for a $c(2 \times 2)$ Ba overlayer on W(001) at different angles of incidence α taken along (a) the $\bar{\Gamma}\Delta\bar{X}$ and (b) the $\bar{\Gamma}\Sigma\bar{M}$ directions of the SBZ of clean W(001).

uum level, provided these kinds of states have the potential to couple to the IPS process and can be observed as resonances. We believe that a comparison between theory and experiment for states immediately above the experimental vacuum level is possible in this case, since the position of the calculated states with respect to the Fermi level is found to be insensitive to the separation between the vacuum level and the calculated Fermi level. The final-state energy shifts due to the occupation of the empty electronic levels are found to be small (+0.1 eV).

Figure 4 shows the dispersion of all the observed peaks as a function of k_{\parallel} in the left panel, and the theoretically calculated DOS for a Ba height of 2.38 Å above the W substrate in the right panel. In contrast to s and p surface states that are observed with inverse photoemission for alkali-metal adsorption on transition metals,²⁹⁻³¹ the states in our case do not have free-electron-like dispersions. Instead, all of the observed unoccupied states, with the exception of the one immediately above E_F , seem to possess little or no dispersion as is expected for states with significant d character. Our theoretical analysis reveals that the state immediately above E_F contains a large Ba d contribution near 0.6 eV and a dominating W contribution in its dispersive part up to 1.6 eV.

The peaks located at or below the vacuum level show strong sensitivity to surface contamination and are, therefore, assigned to transitions into Ba and W d surface states, a conclusion which is supported by the calculated cluster DOS. The peak located near 3.4 eV above E_F , on the other hand, changes only slightly as a result of oxygen adsorption. Therefore, we believe that this state comprises a W bulk component. This is consistent with

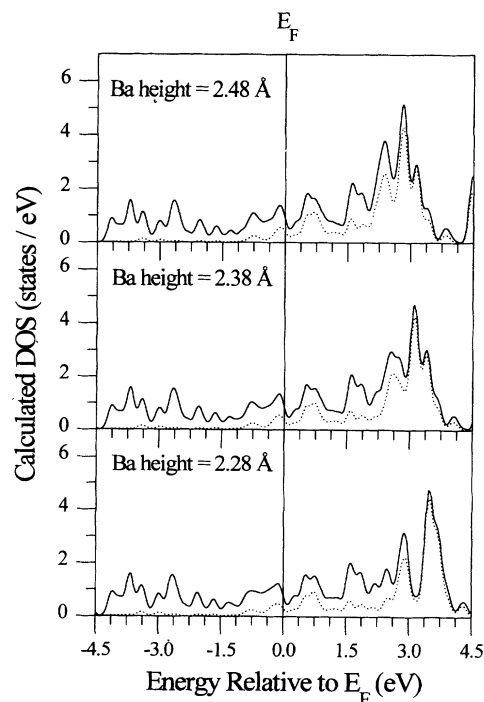


FIG. 3. Fully relativistically calculated DOS for an ordered $c(2 \times 2)$ Ba adlayer on W(001) for three different Ba heights above the surface. The total DOS are represented by solid lines and the Ba contributions by dotted lines.

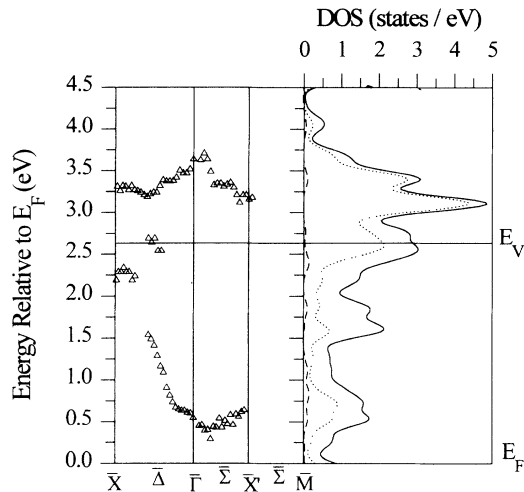


FIG. 4. Left panel: Experimental two-dimensional band structure for a $c(2 \times 2)$ Ba overlayer on W(001) along the $\bar{\Gamma} \Delta \bar{X}$ and $\bar{\Gamma} \Sigma \bar{M}$ symmetry lines of the unreconstructed W(001) surface. Right panel: Fully relativistically calculated DOS for a Ba height of 2.38 Å. The solid line represents the total DOS; the dashed and dotted lines represent the Ba $s+p$ and d contributions, respectively.

the DOS from LAPW calculations for a 19-layer W(001) film, which predict a strong feature near 3.5 eV above E_F originating from the inner layers of the film.³² Furthermore, a bulklike state was observed near 3.5 eV in our IPS measurements of the clean unreconstructed tungsten surface. The band from the unreconstructed surface and the one from 1 ML of Ba on W(001) overlap over large segments of the $\bar{\Gamma} \bar{X}$ and $\bar{\Gamma} \bar{M}$ lines.^{16,28} However, recent Ba on W(001) coverage-dependent data³³ taken in the $\bar{\Gamma} \Sigma \bar{M}$ direction for angles close to 35° reveal a Ba-induced feature in the IPS spectra near 3.4 eV, a region where no tungsten unoccupied states are observed.²⁸ We therefore attribute the band near 3.4 eV to transitions into both Ba d and W bulk d states. This is consistent with the DOS based on the present cluster model and also on FLAPW calculations by Hemstreet and Chubb⁸ for a $c(2 \times 2)$ Ba adlayer placed on both sides of a five-layer W(001) film, which show a strong enhancement of the W-related peaks at 3.2 eV after adsorption of barium. Although our IPS measurements appear to indicate that both Ba and W contribute to the state near 3.4 eV above E_F , the cluster DOS seem to attribute this state almost entirely to Ba d orbitals. This apparent discrepancy is due to the fact that the employed cluster contains only two layers of W atoms, none of which is representative of bulk atoms.

Overall, our experimental and theoretical results are in good agreement with the calculations of Hemstreet and Chubb⁸ in that the same features are obtained above the Fermi level. Their calculations confirm that the surface states and resonances of W(001) acquire significant admixture of Ba d surface states in the vicinity of E_F . In close agreement with the cluster results, their calculated DOS show broad peaks around 0.6 and 1.3 eV above E_F . Their dominant Ba-related peak (for a Ba height of 2.48

Å) is located at 2.7 eV and virtually coincides with the cluster result for the same height (cf. Fig. 3). However, in our experimental spectra a peak at this energy appears only as a shoulder of the main peak at 3.5 eV; it is therefore likely that the Ba height of 2.48 Å is slightly too large.

B. BaO on W(001)

The IPS spectra for 1 ML of Ba and O on W(001) along the $\bar{\Gamma} \Delta \bar{X}$ and $\bar{\Gamma} \Sigma \bar{M}$ symmetry lines are shown in Figs. 5(a) and 5(b), respectively. Spectra corresponding

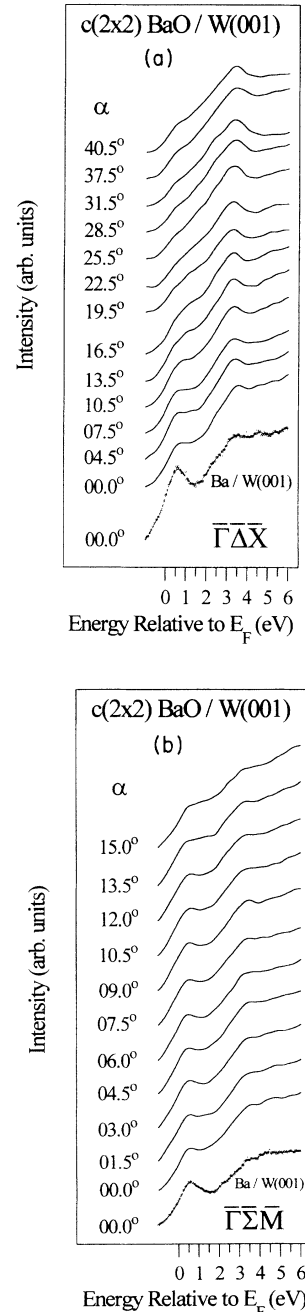


FIG. 5. IPS spectra for a $c(2 \times 2)$ BaO overlayer on W(001) at different angles of incidence α taken along (a) the $\bar{\Gamma} \Delta \bar{X}$ and (b) the $\bar{\Gamma} \Sigma \bar{M}$ directions of the SBZ of clean W(001).

to a $c(2 \times 2)$ Ba monolayer on W(001) taken at normal incidence are shown at the bottom of Figs. 5(a) and 5(b) for comparison. Like the work-function results, the IPS spectra were also independent of the order of Ba and O adsorption on the surface at room temperature. Since IPS is a surface-sensitive technique, this suggests that the arrangement of the adatoms on the surface at room temperature is unique regardless of the order of deposition.

Figure 6 illustrates the fully relativistically calculated cluster DOS for the upright and tilted geometries for the $c(2 \times 2)$ BaO adlayer on W(001). For comparison, we have also included the quasirelativistic DOS (without spin-orbit interaction) for the tilted geometry. Because the fully and quasirelativistic results for the tilted configuration differ significantly, only the fully relativistic treatment is appropriate.

The experimental two-dimensional band structure is presented in Fig. 7 along with the fully relativistically calculated DOS for the tilted configuration. Only two features are observed above E_F for the BaO monolayer. One is located near 0.6 eV and the other near 3.4 eV above E_F , which is 1 eV above E_V .

The agreement with experiment for the lower-energy peaks located at 0.5 and 0.75 eV appears to be better for the upright configuration, as can be seen by comparing Figs. 6 and 7. However, there is a disparity between the experimental results and the DOS for the upright configuration in that the major calculated peak at 1.5 eV is not observed along the two high-symmetry directions ($\bar{\Gamma} \bar{\Delta} \bar{X}$ and $\bar{\Gamma} \bar{\Sigma} \bar{M}$) probed experimentally. Since it is very unlikely that the calculated peak centered around

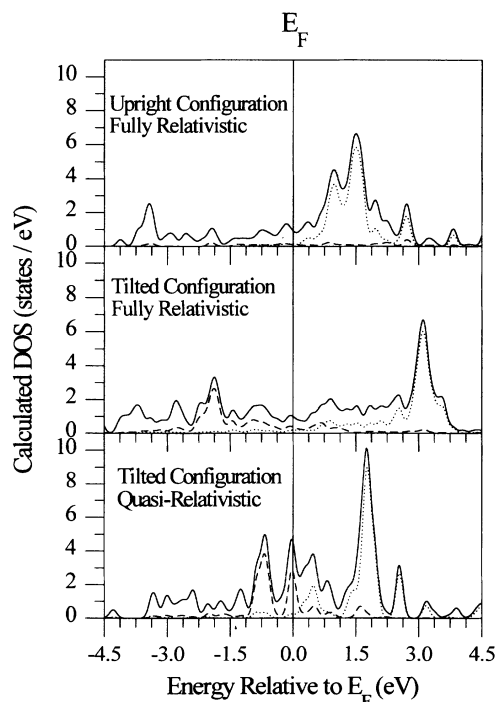


FIG. 6. Quasirelativistically and fully relativistically calculated DOS for a $c(2 \times 2)$ BaO layer on W(001) for two different adsorption configurations (tilted and upright). Solid lines represent the total DOS; dashed and dotted lines represent the oxygen and barium contributions, respectively.

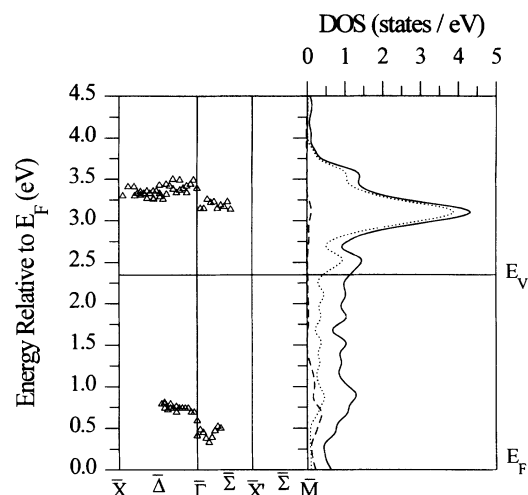


FIG. 7. Left panel: Experimental two-dimensional band structure for a $c(2 \times 2)$ BaO overlayer on W(001) along the $\bar{\Gamma} \bar{\Delta} \bar{X}$ and $\bar{\Gamma} \bar{\Sigma} \bar{M}$ symmetry lines of the unreconstructed W(001) surface. Right panel: Fully relativistically calculated DOS for BaO on W(001) in the tilted configuration. The solid line represents the total DOS; the dashed and dotted lines represent the oxygen and barium contributions, respectively.

1.5 eV has a component that would not be observed experimentally along high-symmetry directions, we believe that the tilted fully relativistic calculation provides the most suitable model. This conclusion is supported by the appearance of a peak in the calculated DOS near the resonance observed experimentally at 3.4 eV.

While the band near 3.4 eV changed only slightly after adsorption of oxygen, which is consistent with this state having a W bulk component, the band near 0.6 eV changed significantly. In contrast to Ba on W(001), the band near 0.6 eV does not disperse in the $\bar{\Gamma} \bar{\Delta} \bar{X}$ direction. It is totally quenched with oxygen adsorption exceeding 1.0 L. IPS data for 0.5 L of oxygen on W(001) reveal several oxygen-induced unoccupied states.³⁴ However, the calculated DOS for 1 ML of BaO on W(001) show only small O contributions in the 0.5–1.0-eV energy range. We believe that the absence of dispersion of the observed Ba states and the relatively small contributions of O unoccupied states above E_F , in the case of Ba and O on the W(001) surface, are the result of electronic charge transfer from W and Ba to O. This charge transfer causes these states to become more localized and, therefore, less dispersive. In addition, a Ba-O surface dipole resulting from the charge transfer from barium to oxygen is created. This dipole opposes and more than compensates for the W-O dipole and is believed to contribute to the net surface dipole responsible for lowering the work function of the surface.

Finally, the nondispersing bands, which were observed for 1 ML of Ba on W(001) at 2.3 and 2.6 eV, are totally quenched after adsorption of O, presumably due to them being moved above the vacuum level as a result of the slight reduction of the work function and due to the consolidation of the different Ba peaks into one major feature in the case of BaO on W (cf. Figs. 4 and 7).

V. SUMMARY AND CONCLUSIONS

The chemisorption of Ba and O on W(001) was studied with inverse photoelectron spectroscopy and relativistic cluster calculations. Adsorption of Ba and BaO created $c(2 \times 2)$ LEED structures at ML coverages. The behavior of the unoccupied electronic states above E_F was investigated at this coverage. It is shown that the observed unoccupied states possess strong Ba d character. The states between 0.5 and 2.5 eV contain contributions from Ba and W surface states. The state near 3.5 eV, which is observed for both Ba and BaO on W(001), is believed to originate from transitions into Ba d surface and W d bulk states.

Oxygen adsorption quenches the Ba/W(001) states located at 2.3 and 2.7 eV and causes the loss of dispersion in the feature near 0.6 eV. This, and the absence of unoccupied O levels, can be explained by electronic charge transfer from Ba and W to O. The additional Ba-O dipole counteracts the W-O dipole, and is believed to be responsible for reducing the work function and enhancing

emission from the BaO/W(001) surface relative to Ba/W(001).

The work function of W(001) ($\phi=4.63$ eV) was reduced to 2.3–2.4 eV upon adsorption of 1 ML of Ba and O. The value of the work function, the LEED structure, and the IPS spectra are independent of the order of Ba and O deposition at this coverage.

Overall, the fully relativistically calculated DOS for $c(2 \times 2)$ Ba and BaO (in the tilted configuration) on W(001) are found to be in reasonably good agreement with the experimental results.

ACKNOWLEDGMENTS

We would like to thank Lou Maschak for his assistance with the experimental setup and Ben Ebihara for designing the Ba source. We would also like to thank Dr. L. A. Hemstreet for sending us a copy of his work on Ba/W(001) before publication. This work was supported by NASA under Contract No. NAS3-25940 and the National Research Council.

-
- ¹G. A. Haas, H. F. Gray, and R. E. Thomas, *J. Appl. Phys.* **46**, 3293 (1975).
²R. Forman, *Appl. Surf. Sci.* **2**, 258 (1979).
³G. A. Haas, A. Shih, and C. R. K. Marrian, *Appl. Surf. Sci.* **16**, 139 (1983).
⁴D. Brion, J. C. Tonnerre, and A. M. Shroff, *Appl. Surf. Sci.* **16**, 55 (1983).
⁵G. A. Haas, C. R. K. Marrian, and A. Shih, *Appl. Surf. Sci.* **24**, 430 (1985).
⁶R. Forman, *J. Appl. Phys.* **47**, 5272 (1976).
⁷G. A. Haas, R. E. Thomas, C. R. K. Marrian, and A. Shih, *Appl. Surf. Sci.* **40**, 277 (1989).
⁸L. A. Hemstreet and S. R. Chubb, *Phys. Rev. B* **47**, 10748 (1993); L. A. Hemstreet (private communication).
⁹E. Wimmer, A. J. Freeman, J. R. Hikes, and A. M. Karo, *Phys. Rev. B* **28**, 3074 (1983).
¹⁰D. M. Riffe, G. K. Wertheim, and P. H. Citrin, *Phys. Rev. Lett.* **64**, 571 (1990).
¹¹D. Norman, R. A. Tuck, H. B. Skinner, P. J. Wadsworth, T. M. Gardiner, I. W. Owen, C. H. Richardson, and G. Thornton, *Phys. Rev. Lett.* **58**, 519 (1987).
¹²G. Thornton, I. W. Owen, C. H. Richardson, D. Norman, R. A. Tuck, H. B. Skinner, P. J. Wadsworth, and T. M. Gardiner, *Vacuum* **38**, 401 (1988).
¹³L. A. Hemstreet, S. R. Chubb, and W. E. Pickett, *Phys. Rev. B* **40**, 3592 (1989); *J. Vac. Sci. Technol. A* **6**, 1063 (1988).
¹⁴A. Shih, C. Hor, W. Elam, J. Kirkland, and D. Mueller, *Phys. Rev. B* **44**, 5818 (1991).
¹⁵W. Müller, *IEEE Trans. Electron Devices* **36**, 180 (1989); *J. Vac. Sci. Technol. A* **6**, 1072 (1988).
¹⁶I. L. Krainsky, *J. Vac. Sci. Technol. A* **5**, 735 (1987).
¹⁷A. Lamouri and I. L. Krainsky, *Surf. Sci.* **278**, 286 (1992).
¹⁸N. Babbe, W. Drube, I. Schäfer, and M. Skibowsky, *J. Phys. E* **18**, 158 (1985).
¹⁹I. L. Krainsky, *Rev. Sci. Instrum.* **62**, 1746 (1991).
²⁰A. Lamouri, I. L. Krainsky, and W. Müller, *Surf. Interface Anal.* **21**, 150 (1994).
²¹R. L. Billington and T. N. Rhodin, *Phys. Rev. B* **41**, 1602 (1978).
²²D. Mueller, A. Shih, E. Roman, T. Madey, R. Kurtz, and R. Stockbauer, *J. Vac. Sci. Technol. A* **6**, 1067 (1988).
²³C. Y. Yang and S. Rabii, *Phys. Rev. A* **12**, 362 (1975).
²⁴C. Y. Yang, *J. Chem. Phys.* **68**, 2626 (1978).
²⁵D. A. Case and C. Y. Yang, *J. Chem. Phys.* **72**, 3443 (1980).
²⁶J. C. Slater, *Adv. Quantum Chem.* **6**, 1 (1972).
²⁷J. G. Norman, Jr., *Mol. Phys.* **31**, 1191 (1976).
²⁸A. Lamouri and I. L. Krainsky, *Surf. Sci.* **303**, 341 (1994).
²⁹W. Jacob, E. Bertel, and V. Dose, *Phys. Rev. B* **35**, 5910 (1987).
³⁰D. Heskett, K. H. Frank, E. E. Koch, and H. J. Freund, *Phys. Rev. B* **36**, 1276 (1987).
³¹R. Dudde, K. H. Frank, and B. Reihl, *Phys. Rev. B* **41**, 4897 (1990).
³²L. F. Mattheiss and D. R. Haman, *Phys. Rev. B* **29**, 5372 (1984).
³³A. Lamouri and I. L. Krainsky (unpublished).
³⁴I. L. Krainsky, *J. Vac. Sci. Technol. A* **6**, 780 (1988).